SCIENCE CHINA
Information Sciences

• RESEARCH PAPER •

November 2017, Vol. 60 112302:1–112302:14
doi: 10.1007/s11432-016-9105-7

Multichannel radar adaptive signal detection in interference and structure nonhomogeneity

Weijian LIU[1], Hui HAN[2], Jun LIU[3,4], Hongli LI[1], Kai LI[5] & Yong-Liang WANG[1*]

[1]*Air Force Early Warning Academy, Wuhan* 430019*, China;*
[2]*State Key Laboratory of Complex Electromagnetic Environment Effects on Electronics and Information System, Luoyang* 471003*, China;*
[3]*National Laboratory of Radar Signal Processing, Xidian University, Xi'an* 710071*, China;*
[4]*Collaborative Innovation Center of Information Sensing and Understanding, Xidian University, Xi'an* 710071*, China;*
[5]*School of Electronic Information, Wuhan University, Wuhan* 430072*, China*

Received November 16, 2016; accepted April 28, 2017; published online September 19, 2017

Abstract In this paper, we consider the problem of multichannel radar signal detection in interference and structure nonhomogeneity. The interference is often caused by electromagnetic countermeasure (ECM) systems or industrial activity, while the nonhomogeneity usually arises because of rapid variations in terrain or radar antenna structure. We propose three adaptive detectors according to three common criteria of detector design, namely, the generalized likelihood ratio test (GLRT), Rao test, and Wald test. Extensive performance comparisons are conducted under different scenarios. It is shown that when the nonhomogeneity is severe, the detector devised according to the GLRT achieves the best detection performance. In other scenarios, the detector designed according to the Wald test may be the best choice, which has the highest probability of detection.

Keywords adaptive detection, generalized likelihood ratio test, heterogeneity, interference, multichannel signal, nonhomogeneity, Rao test, Wald test

Citation Liu W J, Han H, Liu J, et al. Multichannel radar adaptive signal detection in interference and structure nonhomogeneity. Sci China Inf Sci, 2017, 60(11): 112302, doi: 10.1007/s11432-016-9105-7

1 Introduction

Target detection is one of the most important functions of a radar system. Phased-array radar can jointly process multiple spatial and/or temporal data. Hence, the received data are usually multichannel. Compared with single-channel data, the multichannel data contain more information, which can be used to achieve better parameter estimation, target detection, etc. Adaptive multichannel signal detection was first investigated by Kelly [1]. According to the criterion of generalized likelihood ratio test (GLRT), Kelly proposed his famous detector, denoted here as Kelly's GLRT (KGLRT) for convenience. For the same detection problem as in [1], the adaptive matched filter (AMF) detector was independently proposed in [2, 3], both according to the two-step GLRT criterion. Compared with the KGLRT, the AMF has slightly worse detection performance. However, the AMF has lower complexity. In [4], it was shown that

* Corresponding author (email: ylwangkjld@163.com)

the AMF can also be obtained by the criterion of Wald test. The corresponding Rao test was derived in [5] by De Maio, denoted here as De Maio's Rao (DMRao) test. The DMRao test exhibits better performance in terms of the rejection of mismatched signals. The KGLRT, AMF, and DMRao were generalized for subspace signals in [6–8], respectively. Other detection problems include maneuvering target detection [9–12], and so on.

Remarkably, most of the aforementioned detectors were proposed for homogeneous environments, for which the noise in the test and training data share the same covariance matrix. However, the received data usually exhibit different statistical properties due to environmental and instrumental factors. The two main types of nonhomogeneity (or heterogeneity) for the data are power nonhomogeneity and structure nonhomogeneity. For the power nonhomogeneity, the noise in the test data and training data share the same covariance matrix up to a scaling factor, which may be deterministic or random. For the structure nonhomogeneity, the noise covariance matrices in the test and training data do not have the same structure. In particular, partial homogeneity is a kind of power nonhomogeneity, for which the noise in the test and training data share the same covariance matrix up to a deterministic unknown scaling factor. It was pointed out in [13] that the model of partial homogeneity is very suitable for the airborne radar. In [14] the adaptive cosine estimator (ACE) was proposed according to the GLRT criterion. It was shown in [15] that the ACE coincides with the detectors designed by the Rao and Wald tests. The ACE was generalized in [16] for subspace signals and in [17] for double subspace signals. Another kind of power nonhomogeneity is the compound-Gaussian model [18, 19]. In the compound-Gaussian model, clutter is modeled as the product of a complex Gaussian process (referred to as speckle) and a nonnegative scalar (referred to as spiky) that has a much longer decorrelation time than the former. Many detectors in compound-Gaussian clutter are designed under different scenarios, e.g., [20–27] and the references therein.

A type of structure nonhomogeneity is related with the Bayesian model. Precisely, the covariance matrices in the test and training data both assumed to be random, with some joint distribution [28]. Another type of structure nonhomogeneity is caused by random interference. The GLRT in the structure nonhomogeneity, caused by the undernulled random interference, is shown to be the same as the ACE, while the Rao test that was derived in [29] is referred to as the double-normalized AMF (DN-AMF). A similar kind of structure nonhomogeneity is investigated in [30], where the random interference is constrained by the generalized eigen-relation (GER). It was shown that the GLRT shares the same form as the KGLRT, while the Rao test was found to share the same form as the DMRao and the Wald test was identical to the AMF [31].

Remarkably, beside the nonhomogeneity, another severe scenario is directional interference, which may be caused by stand-off jamming (SOJ) or civil broadcasting. In [32] the detection problem in directional interference was considered, where the directional interference was assumed to lie in a known subspace but with unknown coordinates. Several GLRT-based detectors were proposed therein. The detection problem in [32] was generalized in [33] when the subspace containing the directional interference was unknown, and it was solved in an *ad hoc* algorithm strongly related to the GLRT. Liu et al. [34] investigated the detection problem in completely unknown directional interference and two detectors are proposed, namely, the adaptive orthogonal rejection detector (AORD) and adaptive oblique projection detector (AOPD). The statistical performance of the AORD was exploited in [35].

To the best of the authors' knowledge, few researches have considered the simultaneous existence of nonhomogeneity and directional interference. Particularly, Bandiera et al. [36] and Liu et al. [37] considered the detection problem in partial homogeneity and directional interference, and the GLRT-based and Rao test-based detectors were derived, respectively. The detection problem in compound-Gaussian power nonhomogeneity and directional interference was investigated in [38], where a detector was proposed based on the two-step GLRT criterion. Different from the power nonhomogeneity investigated in [36–38], in this paper we consider the problem of target detection in structure nonhomogeneity and directional interference, where the structure nonhomogeneity is caused by undernulled random interference. We propose three adaptive detectors and compare their detection performance. The three detectors are obtained

according to the GLRT, Rao test, and Wald test[1)] [37, 39–41]. Extensive performance evaluations are conducted to compare the detection performance of the proposed detectors.

The rest of this paper is organized as follows. Section 2 gives the problem formulation. Section 3 presents the detector design. Numerical examples are given in Section 4. Finally, conclusion is summarized in Section 5.

2 Problem formulation

Denote the test data by an $N \times 1$ vector $\boldsymbol{x}$, which can be in the spatial, temporal, or spatial-temporal domain. Under hypothesis H_1, $\boldsymbol{x}$ contains signal $\boldsymbol{s}$, directional interference $\boldsymbol{j}$, and noise $\boldsymbol{n}$. It is assumed that $\boldsymbol{s}$ and noise $\boldsymbol{j}$ lie in two linearly independent subspaces. Hence, we have

$$\boldsymbol{s} = \boldsymbol{H}\boldsymbol{\theta} \tag{1}$$

and

$$\boldsymbol{j} = \boldsymbol{J}\boldsymbol{\phi}. \tag{2}$$

The $N \times p$ matrix $\boldsymbol{H}$ and $N \times r$ matrix $\boldsymbol{J}$ span the spaces where $\boldsymbol{s}$ and $\boldsymbol{j}$ lie, respectively, and the $p \times 1$ vector $\boldsymbol{\theta}$ and $r \times 1$ vector $\boldsymbol{\phi}$ are the corresponding coordinates. Moreover, the noise $\boldsymbol{n}$, containing thermal noise and clutter, is ruled by a complex circular Gaussian distribution with mean zero and covariance matrix $\boldsymbol{R}_t$. Under hypothesis H_0, $\boldsymbol{x}$ contains directional interference $\boldsymbol{j}$ and noise $\boldsymbol{n}$. The noise covariance matrix $\boldsymbol{R}_t$ is usually unknown and, hence, a set of training data is needed.

Suppose there are L independent and identically distributed (IID) training data, denoted as $\boldsymbol{x}_l$, $l = 1, \ldots, L$. Here $\boldsymbol{x}_l$ is signal-free and only contains noise $\boldsymbol{n}_l$, and $\boldsymbol{n}_l$ is ruled by a complex circular Gaussian distribution with mean zero and covariance matrix $\boldsymbol{R}$. We consider the structure nonhomogeneity, for which there is structure mismatch between $\boldsymbol{R}_t$ and $\boldsymbol{R}$. In particular, it is assumed that $\boldsymbol{R}_t$ has the form [42]

$$\boldsymbol{R}_t = \boldsymbol{R} + \boldsymbol{q}\boldsymbol{q}^{\mathrm{H}}, \tag{3}$$

where $\boldsymbol{q}$ is an $N \times 1$ vector, denoting the structure mismatch between $\boldsymbol{R}_t$ and $\boldsymbol{R}$. In summary, the detection problem can be formulated by the following binary hypothesis test

$$\begin{cases} H_0 : \begin{cases} \boldsymbol{x} = \boldsymbol{J}\boldsymbol{\phi} + \boldsymbol{n}, \\ \boldsymbol{x}_l = \boldsymbol{n}_l, \quad l = 1, \ldots, L, \end{cases} \\ H_1 : \begin{cases} \boldsymbol{x} = \boldsymbol{H}\boldsymbol{\theta} + \boldsymbol{J}\boldsymbol{\phi} + \boldsymbol{n}, \\ \boldsymbol{x}_l = \boldsymbol{n}_l, \quad l = 1, \ldots, L, \end{cases} \end{cases} \tag{4}$$

where $\boldsymbol{H}$ and $\boldsymbol{J}$ are known and $\boldsymbol{\theta}$, $\boldsymbol{\phi}$, $\boldsymbol{R}$, and $\boldsymbol{q}$ are unknown.

3 Detector design

There are three common criteria for detector design, namely, the GLRT, Rao test, and Wald test. In this section, we devise three adaptive detectors according to these criteria.

3.1 GLRT-based detector

The GLRT criterion can be expressed by

$$t_{\mathrm{GLRT}} = \frac{\max_{\boldsymbol{\theta},\boldsymbol{\phi},\boldsymbol{R},\boldsymbol{q}} f_1(\boldsymbol{x}, \boldsymbol{X}_L)}{\max_{\boldsymbol{\phi},\boldsymbol{R},\boldsymbol{q}} f_0(\boldsymbol{x}, \boldsymbol{X}_L)}, \tag{5}$$

1) Note that in addition to the GLRT criterion, the other two common criteria for detector design are the Rao and Wald tests. Recently, many detectors have been proposed in the literature for different kinds of problems, such as [37, 39–41].

where $f_\tau(\boldsymbol{x}, \boldsymbol{X}_L)$ is the joint probability density function (PDF) of $\boldsymbol{x}$ and $\boldsymbol{X}_L$ under hypothesis H_τ, $\tau = 0,\ 1$. Here $\boldsymbol{X}_L = [\boldsymbol{x}_1, \boldsymbol{x}_2, \ldots, \boldsymbol{x}_L]$ are the training data matrix. The joint PDF of $\boldsymbol{x}$ and $\boldsymbol{X}_L$ under hypothesis H_τ is

$$f_\tau(\boldsymbol{x}, \boldsymbol{X}_L) = \frac{\exp[-\boldsymbol{x}_\tau^{\mathrm{H}}(\boldsymbol{R} + \boldsymbol{q}\boldsymbol{q}^{\mathrm{H}})^{-1}\boldsymbol{x}_\tau - \mathrm{tr}(\boldsymbol{R}^{-1}\boldsymbol{S})]}{\pi^{N(L+1)}|\boldsymbol{R}|^{L+1}}, \tag{6}$$

where

$$\boldsymbol{S} = \boldsymbol{X}_L\boldsymbol{X}_L^{\mathrm{H}} \tag{7}$$

is the L times sample covariance matrix (SCM) and

$$\boldsymbol{x}_\tau = \boldsymbol{x} - \tau\boldsymbol{H}\boldsymbol{\theta} - \boldsymbol{J}\boldsymbol{\phi}. \tag{8}$$

According to the matrix inversion lemma, we have

$$(\boldsymbol{R} + \boldsymbol{q}\boldsymbol{q}^{\mathrm{H}})^{-1} = \boldsymbol{R}^{-1} - \frac{\boldsymbol{R}^{-1}\boldsymbol{q}\boldsymbol{q}^{\mathrm{H}}\boldsymbol{R}^{-1}}{1 + \boldsymbol{q}^{\mathrm{H}}\boldsymbol{R}^{-1}\boldsymbol{q}}. \tag{9}$$

Substituting (9) into (6) leads to

$$f_\tau(\boldsymbol{x}, \boldsymbol{X}_L) = \frac{\exp\{-\mathrm{tr}[\boldsymbol{R}^{-1}(\boldsymbol{S} + \boldsymbol{x}_\tau\boldsymbol{x}_\tau^{\mathrm{H}})]\}}{\pi^{N(L+1)}|\boldsymbol{R}|^{L+1}(1 + \boldsymbol{q}^{\mathrm{H}}\boldsymbol{R}^{-1}\boldsymbol{q})} \exp\left[\frac{|\boldsymbol{x}_\tau^{\mathrm{H}}\boldsymbol{R}^{-1}\boldsymbol{q}|^2}{(1 + \boldsymbol{q}^{\mathrm{H}}\boldsymbol{R}^{-1}\boldsymbol{q})}\right]. \tag{10}$$

Using the results in [42], we can obtain that the maximum likelihood estimators (MLEs) of $\boldsymbol{R}$ and $\boldsymbol{q}$ have the forms

$$\hat{\boldsymbol{R}}_\tau = \frac{1}{L+1}\left(\boldsymbol{S} + \frac{\boldsymbol{x}_\tau\boldsymbol{x}_\tau^{\mathrm{H}}}{L\boldsymbol{x}_\tau^{\mathrm{H}}\boldsymbol{S}^{-1}\boldsymbol{x}_\tau}\right) \tag{11}$$

and

$$\hat{\boldsymbol{q}}_\tau = \gamma_\tau\boldsymbol{x}_\tau, \tag{12}$$

respectively, where γ_τ satisfies

$$|\gamma_\tau|^2 = \frac{\boldsymbol{x}_\tau^{\mathrm{H}}\hat{\boldsymbol{R}}_\tau^{-1}\boldsymbol{x}_\tau - 1}{\boldsymbol{x}_\tau^{\mathrm{H}}\hat{\boldsymbol{R}}_\tau^{-1}\boldsymbol{x}_\tau}. \tag{13}$$

Substituting (11)–(13) into (10) yields

$$f_\tau(\boldsymbol{x}, \boldsymbol{X}_L; \hat{\boldsymbol{q}}_\tau) = \frac{\exp\{-\mathrm{tr}[\boldsymbol{R}^{-1}(\boldsymbol{S} + \boldsymbol{x}_\tau\boldsymbol{x}_\tau^{\mathrm{H}})]\}}{\pi^{N(L+1)}|\boldsymbol{R}|^{L+1}\boldsymbol{x}_\tau^{\mathrm{H}}\boldsymbol{R}^{-1}\boldsymbol{x}_\tau} \exp\left[\boldsymbol{x}_\tau^{\mathrm{H}}\boldsymbol{R}^{-1}\boldsymbol{x}_\tau - 1\right]. \tag{14}$$

Moreover, it follows from (11) that

$$\hat{\boldsymbol{R}}_\tau^{-1} = (L+1)\left[\boldsymbol{S}^{-1} - \frac{\boldsymbol{S}^{-1}\boldsymbol{x}_\tau\boldsymbol{x}_\tau^{\mathrm{H}}\boldsymbol{S}^{-1}}{(L+1)\boldsymbol{x}_\tau^{\mathrm{H}}\boldsymbol{S}^{-1}\boldsymbol{x}_\tau}\right] \tag{15}$$

and

$$|\hat{\boldsymbol{R}}_\tau| = \frac{|\boldsymbol{S}|}{L(L+1)^{N-1}}. \tag{16}$$

Substituting (15) and (16) into (14) results in

$$f_\tau(\boldsymbol{x}, \boldsymbol{X}_L; \hat{\boldsymbol{q}}_\tau, \hat{\boldsymbol{R}}_\tau) = c\big(|\boldsymbol{S}|^{L+1}\boldsymbol{x}_\tau^{\mathrm{H}}\boldsymbol{S}^{-1}\boldsymbol{x}_\tau\big)^{-1}, \tag{17}$$

where $c = L^L(L+1)^{(N-1)(L+1)}/(\mathrm{e}\pi)^{N(L+1)}$. Hence, the GLRT detector can be written as

$$t_{\mathrm{GLRT}} = \frac{\max_{\boldsymbol{\phi}}\boldsymbol{x}_0^{\mathrm{H}}\boldsymbol{S}^{-1}\boldsymbol{x}_0}{\max_{\boldsymbol{\theta},\boldsymbol{\phi}}\boldsymbol{x}_1^{\mathrm{H}}\boldsymbol{S}^{-1}\boldsymbol{x}_1}, \tag{18}$$

where $\boldsymbol{x}_1$ and $\boldsymbol{x}_0$ denote the test data under hypotheses H_1 and H_0, respectively. According to (8), we have

$$\boldsymbol{x}_0 = \boldsymbol{x} - \boldsymbol{J}\boldsymbol{\phi} \tag{19}$$

and

$$\boldsymbol{x}_1 = \boldsymbol{x} - \boldsymbol{B}\boldsymbol{\varphi}, \tag{20}$$

where

$$\boldsymbol{B} = [\boldsymbol{H}, \boldsymbol{J}], \tag{21}$$

$$\boldsymbol{\varphi} = [\boldsymbol{\theta} \;\; \boldsymbol{\phi}]^{\mathrm{T}}. \tag{22}$$

To derive the MLEs of $\boldsymbol{\theta}$ and $\boldsymbol{\phi}$ under hypothesis H_1, we construct the cost function

$$g(\boldsymbol{\varphi}) = (\boldsymbol{x} - \boldsymbol{B}\boldsymbol{\varphi})^{\mathrm{H}} \boldsymbol{S}^{-1} (\boldsymbol{x} - \boldsymbol{B}\boldsymbol{\varphi}). \tag{23}$$

Setting the derivative of (23) with respect to $\boldsymbol{\varphi}$ to be zero, leads to the MLE of $\boldsymbol{\varphi}$ under hypothesis H_1 as

$$\hat{\boldsymbol{\varphi}}_1 = (\boldsymbol{B}^{\mathrm{H}} \boldsymbol{S}^{-1} \boldsymbol{B})^{-1} \boldsymbol{B}^{\mathrm{H}} \boldsymbol{S}^{-1} \boldsymbol{x}. \tag{24}$$

Adopting the same method, we have the MLE of $\boldsymbol{\phi}$ under hypothesis H_0 as

$$\hat{\boldsymbol{\phi}}_0 = (\boldsymbol{J}^{\mathrm{H}} \boldsymbol{S}^{-1} \boldsymbol{J})^{-1} \boldsymbol{J}^{\mathrm{H}} \boldsymbol{S}^{-1} \boldsymbol{x}. \tag{25}$$

Substituting (24) and (25) into (18) results in the GLRT as

$$t_{\mathrm{GLRT}} = \frac{\boldsymbol{x}^{\mathrm{H}} \boldsymbol{S}^{-1} \boldsymbol{x} - \boldsymbol{x}^{\mathrm{H}} \boldsymbol{S}^{-1} \boldsymbol{J} (\boldsymbol{J}^{\mathrm{H}} \boldsymbol{S}^{-1} \boldsymbol{J})^{-1} \boldsymbol{J}^{\mathrm{H}} \boldsymbol{S}^{-1} \boldsymbol{x}}{\boldsymbol{x}^{\mathrm{H}} \boldsymbol{S}^{-1} \boldsymbol{x} - \boldsymbol{x}^{\mathrm{H}} \boldsymbol{S}^{-1} \boldsymbol{B} (\boldsymbol{B}^{\mathrm{H}} \boldsymbol{S}^{-1} \boldsymbol{B})^{-1} \boldsymbol{B}^{\mathrm{H}} \boldsymbol{S}^{-1} \boldsymbol{x}}. \tag{26}$$

The GLRT in (26) can be rewritten in the following compact form:

$$t_{\mathrm{GLRT}} = \frac{\tilde{\boldsymbol{x}}^{\mathrm{H}} \boldsymbol{P}_{\tilde{\boldsymbol{J}}}^{\perp} \tilde{\boldsymbol{x}}}{\tilde{\boldsymbol{x}}^{\mathrm{H}} \boldsymbol{P}_{\tilde{\boldsymbol{B}}}^{\perp} \tilde{\boldsymbol{x}}}, \tag{27}$$

where $\tilde{\boldsymbol{x}} = \boldsymbol{S}^{-1/2}\boldsymbol{x}$, $\tilde{\boldsymbol{J}} = \boldsymbol{S}^{-1/2}\boldsymbol{J}$, $\tilde{\boldsymbol{B}} = \boldsymbol{S}^{-1/2}\boldsymbol{B}$, $\boldsymbol{P}_{\tilde{\boldsymbol{J}}}^{\perp} = \boldsymbol{I}_N - \boldsymbol{P}_{\tilde{\boldsymbol{J}}}$, $\boldsymbol{P}_{\tilde{\boldsymbol{J}}} = \tilde{\boldsymbol{J}}(\tilde{\boldsymbol{J}}^{\mathrm{H}}\tilde{\boldsymbol{J}})^{-1}\tilde{\boldsymbol{J}}^{\mathrm{H}}$, $\boldsymbol{P}_{\tilde{\boldsymbol{B}}}^{\perp} = \boldsymbol{I}_N - \boldsymbol{P}_{\tilde{\boldsymbol{B}}}$, and $\boldsymbol{P}_{\tilde{\boldsymbol{B}}} = \tilde{\boldsymbol{B}}(\tilde{\boldsymbol{B}}^{\mathrm{H}}\tilde{\boldsymbol{B}})^{-1}\tilde{\boldsymbol{B}}^{\mathrm{H}}$. Moreover, using the identity $\boldsymbol{P}_{\tilde{\boldsymbol{B}}} = \boldsymbol{P}_{\tilde{\boldsymbol{J}}} + \boldsymbol{P}_{\boldsymbol{P}_{\tilde{\boldsymbol{J}}}^{\perp}\tilde{\boldsymbol{H}}}$ [43, p.54], we have

$$\boldsymbol{P}_{\tilde{\boldsymbol{B}}}^{\perp} = \boldsymbol{P}_{\tilde{\boldsymbol{J}}}^{\perp} - \boldsymbol{P}_{\boldsymbol{P}_{\tilde{\boldsymbol{J}}}^{\perp}\tilde{\boldsymbol{H}}}. \tag{28}$$

According to (28), the GLRT in (27) can be rewritten in the following equivalent form:

$$t'_{\mathrm{GLRT}} = \frac{\tilde{\boldsymbol{x}}^{\mathrm{H}} \boldsymbol{P}_{\boldsymbol{P}_{\tilde{\boldsymbol{J}}}^{\perp}\tilde{\boldsymbol{H}}} \tilde{\boldsymbol{x}}}{\tilde{\boldsymbol{x}}^{\mathrm{H}} \boldsymbol{P}_{\tilde{\boldsymbol{J}}}^{\perp} \tilde{\boldsymbol{x}}}. \tag{29}$$

It is worth pointing out that the GLRT in (29) shares the same form as the GLRT in [36], which is devised in partial homogeneity and directional interference.

3.2 Rao test-based detector

Let $\boldsymbol{\Theta}$ be an $(N^2 + N + p + r) \times 1$ vector in the form

$$\boldsymbol{\Theta} = [\boldsymbol{\Theta}_{\boldsymbol{r}}^{\mathrm{T}}, \boldsymbol{\Theta}_{\boldsymbol{s}}^{\mathrm{T}}]^{\mathrm{T}} = [\boldsymbol{\theta}^{\mathrm{T}}, \boldsymbol{\phi}^{\mathrm{T}}, \boldsymbol{q}^{\mathrm{T}}, \mathrm{vec}^{\mathrm{T}}(\boldsymbol{R})]^{\mathrm{T}}, \tag{30}$$

where $\boldsymbol{\Theta}_r = \boldsymbol{\theta} \in \mathbb{C}^{p\times 1}$, $\boldsymbol{\Theta}_s = [\boldsymbol{\phi}^{\mathrm{T}}, \boldsymbol{q}^{\mathrm{T}}, \mathrm{vec}^{\mathrm{T}}(\boldsymbol{R})]^{\mathrm{T}} \in \mathbb{C}^{(N^2+N+r)\times 1}$, the notation $\mathrm{vec}(\cdot)$ stands for the vectorization operation. Usually, $\boldsymbol{\Theta}_r$ and $\boldsymbol{\Theta}_s$ are called the relative parameter and nuisance parameter, respectively. For the complex circular parameter, the Fisher information matrix (FIM) is [44]

$$\boldsymbol{I}(\boldsymbol{\Theta}) = \mathrm{E}\left[\left(\frac{\partial \ln f_1(\boldsymbol{x}, \boldsymbol{X}_L)}{\partial \boldsymbol{\Theta}^*}\right)\left(\frac{\partial \ln f_1(\boldsymbol{x}, \boldsymbol{X}_L)}{\partial \boldsymbol{\Theta}}\right)^{\mathrm{T}}\right]. \tag{31}$$

For convenience, we can partition the FIM as

$$\boldsymbol{I}(\boldsymbol{\Theta}) = \begin{bmatrix} \boldsymbol{I}_{\boldsymbol{\Theta}_r\boldsymbol{\Theta}_r} & \boldsymbol{I}_{\boldsymbol{\Theta}_r\boldsymbol{\Theta}_s} \\ \boldsymbol{I}_{\boldsymbol{\Theta}_s\boldsymbol{\Theta}_r} & \boldsymbol{I}_{\boldsymbol{\Theta}_s\boldsymbol{\Theta}_s} \end{bmatrix}. \tag{32}$$

Then, the Rao test can be expressed as [44]

$$t_{\mathrm{Rao}} = \left.\frac{\partial \ln f_1(\boldsymbol{x}, \boldsymbol{X}_L)}{\partial \boldsymbol{\Theta}_r^*}\right|_{\boldsymbol{\Theta}=\widehat{\boldsymbol{\Theta}}_0}^{\mathrm{T}} [\boldsymbol{I}^{-1}(\widehat{\boldsymbol{\Theta}}_0)]_{\boldsymbol{\Theta}_r\boldsymbol{\Theta}_r} \left.\frac{\partial \ln f_1(\boldsymbol{x}, \boldsymbol{X}_L)}{\partial \boldsymbol{\Theta}_r^*}\right|_{\boldsymbol{\Theta}=\widehat{\boldsymbol{\Theta}}_0}, \tag{33}$$

where $\hat{\boldsymbol{\Theta}}_0 = [\hat{\boldsymbol{\Theta}}_{r0}, \hat{\boldsymbol{\Theta}}_{s0}^{\mathrm{T}}]^{\mathrm{T}}$ is the MLE of $\boldsymbol{\Theta}$ under hypothesis H_0,

$$[\boldsymbol{I}^{-1}(\boldsymbol{\Theta})]_{\boldsymbol{\Theta}_r\boldsymbol{\Theta}_r} = [\boldsymbol{I}_{\boldsymbol{\Theta}_r\boldsymbol{\Theta}_r}(\boldsymbol{\Theta}) - \boldsymbol{I}_{\boldsymbol{\Theta}_r\boldsymbol{\Theta}_s}(\boldsymbol{\Theta})\boldsymbol{I}_{\boldsymbol{\Theta}_s\boldsymbol{\Theta}_s}^{-1}(\boldsymbol{\Theta})\boldsymbol{I}_{\boldsymbol{\Theta}_s\boldsymbol{\Theta}_r}(\boldsymbol{\Theta})]^{-1}. \tag{34}$$

Using (6), we have

$$\frac{\partial \ln f_1(\boldsymbol{x}, \boldsymbol{X}_L)}{\partial \boldsymbol{\theta}} = \{(\boldsymbol{x} - \boldsymbol{H}\boldsymbol{\theta} - \boldsymbol{J}\boldsymbol{\phi})^{\mathrm{H}}(\boldsymbol{R} + \boldsymbol{q}\boldsymbol{q}^{\mathrm{H}})^{-1}\boldsymbol{H}\}^{\mathrm{T}}. \tag{35}$$

Nulling the derivative of (35) with respect to $\boldsymbol{\theta}^*$ leads to

$$\frac{\partial^2 \ln f_1(\boldsymbol{x}, \boldsymbol{X}_L)}{\partial \boldsymbol{\theta}\partial \boldsymbol{\theta}^*} = -\boldsymbol{H}^{\mathrm{H}}(\boldsymbol{R} + \boldsymbol{q}\boldsymbol{q}^{\mathrm{H}})^{-1}\boldsymbol{H}. \tag{36}$$

According to $\boldsymbol{I}_{\boldsymbol{\Theta}_r\boldsymbol{\Theta}_r}(\boldsymbol{\Theta}) = -\partial^2 \ln f/\partial\boldsymbol{\theta}\partial\boldsymbol{\theta}^*$, we obtain

$$\boldsymbol{I}_{\boldsymbol{\Theta}_r\boldsymbol{\Theta}_r}(\boldsymbol{\Theta}) = \boldsymbol{H}^{\mathrm{H}}(\boldsymbol{R} + \boldsymbol{q}\boldsymbol{q}^{\mathrm{H}})^{-1}\boldsymbol{H}. \tag{37}$$

It is easy to verify that $\boldsymbol{I}_{\boldsymbol{\Theta}_r\boldsymbol{\Theta}_s}(\boldsymbol{\Theta})$ and $\boldsymbol{I}_{\boldsymbol{\Theta}_s\boldsymbol{\Theta}_r}(\boldsymbol{\Theta})$ are zero matrices. It follows that

$$[\boldsymbol{I}^{-1}(\boldsymbol{\Theta})]_{\boldsymbol{\Theta}_r\boldsymbol{\Theta}_r} = \boldsymbol{I}_{\boldsymbol{\Theta}_r\boldsymbol{\Theta}_r}^{-1}(\boldsymbol{\Theta}) = \left[\boldsymbol{H}^{\mathrm{H}}(\boldsymbol{R} + \boldsymbol{q}\boldsymbol{q}^{\mathrm{H}})^{-1}\boldsymbol{H}\right]^{-1}. \tag{38}$$

Taking (35) and (38) into (33) yields the Rao test for given $\boldsymbol{\phi}$, $\boldsymbol{R}$, and $\boldsymbol{q}$, described as

$$t_{\mathrm{Rao}_{\boldsymbol{\phi},\boldsymbol{R},\boldsymbol{q}}} = \boldsymbol{x}_0^{\mathrm{H}}(\boldsymbol{R} + \boldsymbol{q}\boldsymbol{q}^{\mathrm{H}})^{-1}\boldsymbol{H}\left[\boldsymbol{H}^{\mathrm{H}}(\boldsymbol{R} + \boldsymbol{q}\boldsymbol{q}^{\mathrm{H}})^{-1}\boldsymbol{H}\right]^{-1}\boldsymbol{H}^{\mathrm{H}}(\boldsymbol{R} + \boldsymbol{q}\boldsymbol{q}^{\mathrm{H}})^{-1}\boldsymbol{x}_0, \tag{39}$$

where we have used the fact that $\boldsymbol{\theta} = \boldsymbol{0}_{p\times 1}$ and $\boldsymbol{x}_0$ are given in (9) under hypothesis H_0.

To obtain the final Rao test, we need to obtain the MLEs of $\boldsymbol{\phi}$, $\boldsymbol{q}$, and $\boldsymbol{R}$ under hypothesis H_0. In view of (9), we have

$$\begin{aligned}\left[\boldsymbol{H}^{\mathrm{H}}(\boldsymbol{R} + \boldsymbol{q}\boldsymbol{q}^{\mathrm{H}})^{-1}\boldsymbol{H}\right]^{-1} &= \left[\boldsymbol{H}^{\mathrm{H}}\boldsymbol{R}^{-1}\boldsymbol{H} - \frac{\boldsymbol{H}^{\mathrm{H}}\boldsymbol{R}^{-1}\boldsymbol{q}\boldsymbol{q}^{\mathrm{H}}\boldsymbol{R}^{-1}\boldsymbol{H}}{1 + \boldsymbol{q}^{\mathrm{H}}\boldsymbol{R}^{-1}\boldsymbol{q}}\right]^{-1} \\ &= (\boldsymbol{H}^{\mathrm{H}}\boldsymbol{R}^{-1}\boldsymbol{H})^{-1} + \frac{(\boldsymbol{H}^{\boldsymbol{H}}\boldsymbol{R}^{-1}\boldsymbol{H})^{-1}\boldsymbol{H}^{\mathrm{H}}\boldsymbol{R}^{-1}\boldsymbol{q}\boldsymbol{q}^{\mathrm{H}}\boldsymbol{R}^{-1}\boldsymbol{H}(\boldsymbol{H}^{\mathrm{H}}\boldsymbol{R}^{-1}\boldsymbol{H})^{-1}}{1 + \boldsymbol{q}^{\mathrm{H}}\boldsymbol{R}^{-1}\boldsymbol{q} - \boldsymbol{q}^{\mathrm{H}}\boldsymbol{R}^{-1}\boldsymbol{H}(\boldsymbol{H}^{\mathrm{H}}\boldsymbol{R}^{-1}\boldsymbol{H})^{-1}\boldsymbol{H}^{\mathrm{H}}\boldsymbol{R}^{-1}\boldsymbol{q}}.\end{aligned} \tag{40}$$

Substituting (9) and (40) into (39), after some algebra, yields

$$\begin{aligned}t_{\mathrm{Rao}_{\boldsymbol{\phi},\boldsymbol{R},\boldsymbol{q}}} = {} & \boldsymbol{x}_0^{\mathrm{H}}\left[\boldsymbol{R}^{-1} - \frac{\boldsymbol{R}^{-1}\boldsymbol{q}\boldsymbol{q}^{\mathrm{H}}\boldsymbol{R}^{-1}}{1 + \boldsymbol{q}^{\mathrm{H}}\boldsymbol{R}^{-1}\boldsymbol{q}}\right]\boldsymbol{H} \\ & \cdot \left[(\boldsymbol{H}^{\mathrm{H}}\boldsymbol{R}^{-1}\boldsymbol{H})^{-1} + \frac{(\boldsymbol{H}^{\mathrm{H}}\boldsymbol{R}^{-1}\boldsymbol{H})^{-1}\boldsymbol{H}^{\mathrm{H}}\boldsymbol{R}^{-1}\boldsymbol{q}\boldsymbol{q}^{\mathrm{H}}\boldsymbol{R}^{-1}\boldsymbol{H}(\boldsymbol{H}^{\boldsymbol{H}}\boldsymbol{R}^{-1}\boldsymbol{H})^{-1}}{1 + \boldsymbol{q}^{\mathrm{H}}\boldsymbol{R}^{-1}\boldsymbol{q} - \boldsymbol{q}^{\mathrm{H}}\boldsymbol{R}^{-1}\boldsymbol{H}(\boldsymbol{H}^{\mathrm{H}}\boldsymbol{R}^{-1}\boldsymbol{H})^{-1}\boldsymbol{H}^{\mathrm{H}}\boldsymbol{R}^{-1}\boldsymbol{q}}\right] \\ & \cdot \boldsymbol{H}^{\mathrm{H}}\left[\boldsymbol{R}^{-1} - \frac{\boldsymbol{R}^{-1}\boldsymbol{q}\boldsymbol{q}^{\mathrm{H}}\boldsymbol{R}^{-1}}{1 + \boldsymbol{q}^{\mathrm{H}}\boldsymbol{R}^{-1}\boldsymbol{q}}\right]\boldsymbol{x}_0.\end{aligned} \tag{41}$$

Eq. (41) can be recast as the following compact form:

$$t_{\mathrm{Rao}_{\boldsymbol{\phi},\boldsymbol{R},\boldsymbol{q}}} = \bar{\boldsymbol{x}}_0^{\mathrm{H}} \left[\boldsymbol{I}_N - \frac{\bar{\boldsymbol{q}}\bar{\boldsymbol{q}}^{\mathrm{H}}}{1+\bar{\boldsymbol{q}}^{\mathrm{H}}\bar{\boldsymbol{q}}}\right] \left[\boldsymbol{P}_{\bar{\boldsymbol{H}}} + \frac{\boldsymbol{P}_{\bar{\boldsymbol{H}}}\bar{\boldsymbol{q}}\bar{\boldsymbol{q}}^{\mathrm{H}}\boldsymbol{P}_{\bar{\boldsymbol{H}}}}{1+\bar{\boldsymbol{q}}^{\mathrm{H}}\boldsymbol{P}_{\bar{\boldsymbol{H}}}^{\perp}\bar{\boldsymbol{q}}}\right] \left[\boldsymbol{I}_N - \frac{\bar{\boldsymbol{q}}\bar{\boldsymbol{q}}^{\mathrm{H}}}{1+\bar{\boldsymbol{q}}^{\mathrm{H}}\bar{\boldsymbol{q}}}\right] \bar{\boldsymbol{x}}_0, \tag{42}$$

where $\bar{\boldsymbol{x}}_0 = \boldsymbol{R}^{-1/2}\boldsymbol{x}_0$, $\bar{\boldsymbol{q}} = \boldsymbol{R}^{-1/2}\boldsymbol{q}$, $\bar{\boldsymbol{H}} = \boldsymbol{R}^{-1/2}\boldsymbol{H}$, and $\boldsymbol{P}_{\bar{\boldsymbol{H}}} = \bar{\boldsymbol{H}}(\bar{\boldsymbol{H}}^{\mathrm{H}}\bar{\boldsymbol{H}})^{-1}\bar{\boldsymbol{H}}^{\mathrm{H}}$.

According to (12) and (13), we have

$$\left[\boldsymbol{I}_N - \frac{\bar{\boldsymbol{q}}\bar{\boldsymbol{q}}^{\mathrm{H}}}{1+\bar{\boldsymbol{q}}^{\mathrm{H}}\bar{\boldsymbol{q}}}\right] \bar{\boldsymbol{x}}_0 = \frac{\bar{\boldsymbol{x}}_0}{\bar{\boldsymbol{x}}_0^{\mathrm{H}}\bar{\boldsymbol{x}}_0}. \tag{43}$$

Taking (43) into (42), and using (12) and (13) again, we arrive at

$$t_{\mathrm{Rao}_{\boldsymbol{\phi},\boldsymbol{R}}} = \frac{\bar{\boldsymbol{x}}_0^{\mathrm{H}}\boldsymbol{P}_{\bar{\boldsymbol{H}}}\bar{\boldsymbol{x}}_0}{\bar{\boldsymbol{x}}_0^{\mathrm{H}}\boldsymbol{P}_{\bar{\boldsymbol{H}}}\bar{\boldsymbol{x}}_0 + \bar{\boldsymbol{x}}_0^{\mathrm{H}}\bar{\boldsymbol{x}}_0\bar{\boldsymbol{x}}_0^{\mathrm{H}}\boldsymbol{P}_{\bar{\boldsymbol{H}}}^{\perp}\bar{\boldsymbol{x}}_0}. \tag{44}$$

Dividing both sides of (44) by $\bar{\boldsymbol{x}}_0^{\mathrm{H}}\bar{\boldsymbol{x}}_0$ yields

$$t_{\mathrm{Rao}_{\boldsymbol{\phi},\boldsymbol{R}}} = \frac{\dfrac{\bar{\boldsymbol{x}}_0^{\mathrm{H}}\boldsymbol{P}_{\bar{\boldsymbol{H}}}\bar{\boldsymbol{x}}_0}{\bar{\boldsymbol{x}}_0^{\mathrm{H}}\bar{\boldsymbol{x}}_0}}{\dfrac{\bar{\boldsymbol{x}}_0^{\mathrm{H}}\boldsymbol{P}_{\bar{\boldsymbol{H}}}\bar{\boldsymbol{x}}_0}{\bar{\boldsymbol{x}}_0^{\mathrm{H}}\bar{\boldsymbol{x}}_0} + \bar{\boldsymbol{x}}_0^{\mathrm{H}}\boldsymbol{P}_{\bar{\boldsymbol{H}}}^{\perp}\bar{\boldsymbol{x}}_0}. \tag{45}$$

Eq. (45) is statistically equivalent to

$$t'_{\mathrm{Rao}_{\boldsymbol{\phi},\boldsymbol{R}}} = \frac{\bar{\boldsymbol{x}}_0^{\mathrm{H}}\boldsymbol{P}_{\bar{\boldsymbol{H}}}\bar{\boldsymbol{x}}_0}{\bar{\boldsymbol{x}}_0^{\mathrm{H}}\bar{\boldsymbol{x}}_0\bar{\boldsymbol{x}}_0^{\mathrm{H}}\boldsymbol{P}_{\bar{\boldsymbol{H}}}^{\perp}\bar{\boldsymbol{x}}_0}, \tag{46}$$

owing to the fact that $t_{\mathrm{Rao}_{\boldsymbol{\phi},\boldsymbol{R}}} = [1 + (t'_{\mathrm{Rao}_{\boldsymbol{\phi},\boldsymbol{R}}})^{-1}]^{-1}$ is a monotonically increasing function of $t'_{\mathrm{Rao}_{\boldsymbol{\phi},\boldsymbol{R}}}$.

If we substitute the MLE of $\boldsymbol{R}$ and $\boldsymbol{\phi}$ under hypothesis H_0 into (46), we will find the final Rao test. The detailed derivations are given below. First, extending (46) as follows:

$$t'_{\mathrm{Rao}_{\boldsymbol{\phi},\boldsymbol{R}}} = \frac{\boldsymbol{x}_0^{\mathrm{H}}\boldsymbol{R}^{-1}\boldsymbol{H}^{\mathrm{H}}(\boldsymbol{H}^{\mathrm{H}}\boldsymbol{R}^{-1}\boldsymbol{H})^{-1}\boldsymbol{H}^{\mathrm{H}}\boldsymbol{R}^{-1}\boldsymbol{x}_0}{\boldsymbol{x}_0^{\mathrm{H}}\boldsymbol{R}^{-1}\boldsymbol{x}_0\left[\boldsymbol{x}_0^{\mathrm{H}}\boldsymbol{R}^{-1}\boldsymbol{x}_0 - \boldsymbol{x}_0^{\mathrm{H}}\boldsymbol{R}^{-1}\boldsymbol{H}^{\mathrm{H}}(\boldsymbol{H}^{\mathrm{H}}\boldsymbol{R}^{-1}\boldsymbol{H})^{-1}\boldsymbol{H}^{\mathrm{H}}\boldsymbol{R}^{-1}\boldsymbol{x}_0\right]}. \tag{47}$$

Using (15), we have

$$\hat{\boldsymbol{R}}_0^{-1} = (L+1)\boldsymbol{S}^{-1} - \frac{\boldsymbol{S}^{-1}\boldsymbol{x}_0\boldsymbol{x}_0^{\mathrm{H}}\boldsymbol{S}^{-1}}{\boldsymbol{x}_0^{\mathrm{H}}\boldsymbol{S}^{-1}\boldsymbol{x}_0}. \tag{48}$$

Using (48), we obtain the following three equations:

$$\boldsymbol{x}_0^{\mathrm{H}}\boldsymbol{R}^{-1}\boldsymbol{x}_0 = (L+1)\tilde{\boldsymbol{x}}_0^{\mathrm{H}}\tilde{\boldsymbol{x}}_0 - \tilde{\boldsymbol{x}}_0^{\mathrm{H}}\tilde{\boldsymbol{x}}_0 = L\tilde{\boldsymbol{x}}_0^{\mathrm{H}}\tilde{\boldsymbol{x}}_0, \tag{49}$$

$$\boldsymbol{H}^{\mathrm{H}}\boldsymbol{R}^{-1}\boldsymbol{x}_0 = (L+1)\tilde{\boldsymbol{H}}^{\mathrm{H}}\tilde{\boldsymbol{x}}_0 - \tilde{\boldsymbol{H}}^{\mathrm{H}}\tilde{\boldsymbol{x}}_0 = L\tilde{\boldsymbol{H}}^{\mathrm{H}}\tilde{\boldsymbol{x}}_0, \tag{50}$$

and

$$\begin{aligned}(\boldsymbol{H}^{\mathrm{H}}\boldsymbol{R}^{-1}\boldsymbol{H})^{-1} &= \left[(L+1)\boldsymbol{H}^{\mathrm{H}}\boldsymbol{S}^{-1}\boldsymbol{H} - \frac{\boldsymbol{H}^{\mathrm{H}}\boldsymbol{S}^{-1}\boldsymbol{x}_0\boldsymbol{x}_0^{\mathrm{H}}\boldsymbol{S}^{-1}\boldsymbol{H}}{\boldsymbol{x}_0^{\mathrm{H}}\boldsymbol{S}^{-1}\boldsymbol{x}_0}\right]^{-1} \\ &= \frac{1}{L+1}(\boldsymbol{H}^{\mathrm{H}}\boldsymbol{S}^{-1}\boldsymbol{H})^{-1} + \frac{1}{L+1}\frac{(\boldsymbol{H}^{\mathrm{H}}\boldsymbol{S}^{-1}\boldsymbol{H})^{-1}\boldsymbol{H}^{\mathrm{H}}\boldsymbol{S}^{-1}\boldsymbol{x}_0\boldsymbol{x}_0^{\mathrm{H}}\boldsymbol{S}^{-1}\boldsymbol{H}(\boldsymbol{H}^{\mathrm{H}}\boldsymbol{S}^{-1}\boldsymbol{H})^{-1}}{(L+1)\boldsymbol{x}_0^{\mathrm{H}}\boldsymbol{S}^{-1}\boldsymbol{x}_0 - \boldsymbol{x}_0^{\mathrm{H}}\boldsymbol{S}^{-1}\boldsymbol{H}(\boldsymbol{H}^{\mathrm{H}}\boldsymbol{S}^{-1}\boldsymbol{H})^{-1}\boldsymbol{H}^{\mathrm{H}}\boldsymbol{S}^{-1}\boldsymbol{x}_0} \\ &= \frac{1}{L+1}(\tilde{\boldsymbol{H}}^{\mathrm{H}}\tilde{\boldsymbol{H}})^{-1} + \frac{1}{L+1}\frac{(\tilde{\boldsymbol{H}}^{\mathrm{H}}\tilde{\boldsymbol{H}})^{-1}\tilde{\boldsymbol{H}}^{\mathrm{H}}\tilde{\boldsymbol{x}}_0\tilde{\boldsymbol{x}}_0^{\mathrm{H}}\tilde{\boldsymbol{H}}(\tilde{\boldsymbol{H}}^{\mathrm{H}}\tilde{\boldsymbol{H}})^{-1}}{(L+1)\tilde{\boldsymbol{x}}_0^{\mathrm{H}}\tilde{\boldsymbol{x}}_0 - \tilde{\boldsymbol{x}}_0^{\mathrm{H}}\boldsymbol{P}_{\tilde{\boldsymbol{H}}}\tilde{\boldsymbol{x}}_0^{\mathrm{H}}}.\end{aligned} \tag{51}$$

Substituting (49)–(51) into the numerator of (47) results in

$$\begin{aligned}\boldsymbol{x}_0^{\mathrm{H}}\boldsymbol{R}^{-1}\boldsymbol{H}^{\mathrm{H}}(\boldsymbol{H}^{\mathrm{H}}\boldsymbol{R}^{-1}\boldsymbol{H})^{-1}\boldsymbol{H}^{\mathrm{H}}\boldsymbol{R}^{-1}\boldsymbol{x}_0 &= \frac{L^2}{L+1}\left[\tilde{\boldsymbol{x}}_0^{\mathrm{H}}\boldsymbol{P}_{\tilde{\boldsymbol{H}}}\tilde{\boldsymbol{x}}_0 + \frac{(\tilde{\boldsymbol{x}}_0^{\mathrm{H}}\boldsymbol{P}_{\tilde{\boldsymbol{H}}}\tilde{\boldsymbol{x}}_0)^2}{(L+1)\tilde{\boldsymbol{x}}_0^{\mathrm{H}}\tilde{\boldsymbol{x}}_0 - \tilde{\boldsymbol{x}}_0^{\mathrm{H}}\boldsymbol{P}_{\tilde{\boldsymbol{H}}}\tilde{\boldsymbol{x}}_0^{\mathrm{H}}}\right]\\ &= \frac{L^2\tilde{\boldsymbol{x}}_0^{\mathrm{H}}\tilde{\boldsymbol{x}}_0\tilde{\boldsymbol{x}}_0^{\mathrm{H}}\boldsymbol{P}_{\tilde{\boldsymbol{H}}}\tilde{\boldsymbol{x}}_0}{(L+1)\tilde{\boldsymbol{x}}_0^{\mathrm{H}}\tilde{\boldsymbol{x}}_0 - \tilde{\boldsymbol{x}}_0^{\mathrm{H}}\boldsymbol{P}_{\tilde{\boldsymbol{H}}}\tilde{\boldsymbol{x}}_0^{\mathrm{H}}}.\end{aligned} \tag{52}$$

Taking (49) and (52) into (47), after some algebra, leads to

$$t'_{\mathrm{Rao}_{\boldsymbol{\phi}}} = \frac{\tilde{\boldsymbol{x}}_0^{\mathrm{H}}\boldsymbol{P}_{\tilde{\boldsymbol{H}}}\tilde{\boldsymbol{x}}_0}{(L+1)\tilde{\boldsymbol{x}}_0^{\mathrm{H}}\tilde{\boldsymbol{x}}_0(\tilde{\boldsymbol{x}}_0^{\mathrm{H}}\tilde{\boldsymbol{x}}_0 - \tilde{\boldsymbol{x}}_0^{\mathrm{H}}\boldsymbol{P}_{\tilde{\boldsymbol{H}}}\tilde{\boldsymbol{x}}_0)}, \tag{53}$$

with the constant dropped, we have

$$t''_{\mathrm{Rao}_{\boldsymbol{\phi}}} = \frac{\tilde{\boldsymbol{x}}_0^{\mathrm{H}}\boldsymbol{P}_{\tilde{\boldsymbol{H}}}\tilde{\boldsymbol{x}}_0}{\tilde{\boldsymbol{x}}_0^{\mathrm{H}}\tilde{\boldsymbol{x}}_0(\tilde{\boldsymbol{x}}_0^{\mathrm{H}}\tilde{\boldsymbol{x}}_0 - \tilde{\boldsymbol{x}}_0^{\mathrm{H}}\boldsymbol{P}_{\tilde{\boldsymbol{H}}}\tilde{\boldsymbol{x}}_0)}. \tag{54}$$

Using (25), we have

$$\tilde{\boldsymbol{x}}_0 = \boldsymbol{P}_{\tilde{\boldsymbol{J}}}^{\perp}\tilde{\boldsymbol{x}}, \tag{55}$$

where $\tilde{\boldsymbol{x}} = \boldsymbol{S}^{-1/2}\boldsymbol{x}$. Substituting (55) into (54) yields the final Rao test

$$t_{\mathrm{Rao}} = \frac{\tilde{\boldsymbol{x}}^{\mathrm{H}}\boldsymbol{P}_{\tilde{\boldsymbol{J}}}^{\perp}\boldsymbol{P}_{\tilde{\boldsymbol{H}}}\boldsymbol{P}_{\tilde{\boldsymbol{J}}}^{\perp}\tilde{\boldsymbol{x}}}{\tilde{\boldsymbol{x}}^{\mathrm{H}}\boldsymbol{P}_{\tilde{\boldsymbol{J}}}^{\perp}\tilde{\boldsymbol{x}}(\tilde{\boldsymbol{x}}^{\mathrm{H}}\boldsymbol{P}_{\tilde{\boldsymbol{J}}}^{\perp}\tilde{\boldsymbol{x}} - \tilde{\boldsymbol{x}}^{\mathrm{H}}\boldsymbol{P}_{\tilde{\boldsymbol{J}}}^{\perp}\boldsymbol{P}_{\tilde{\boldsymbol{H}}}\boldsymbol{P}_{\tilde{\boldsymbol{J}}}^{\perp}\tilde{\boldsymbol{x}})}, \tag{56}$$

which can be recast as

$$t_{\mathrm{Rao}} = \frac{\tilde{\boldsymbol{x}}^{\mathrm{H}}\boldsymbol{P}_{\tilde{\boldsymbol{J}}}^{\perp}\boldsymbol{P}_{\tilde{\boldsymbol{H}}}\boldsymbol{P}_{\tilde{\boldsymbol{J}}}^{\perp}\tilde{\boldsymbol{x}}}{\tilde{\boldsymbol{x}}^{\mathrm{H}}\boldsymbol{P}_{\tilde{\boldsymbol{J}}}^{\perp}\tilde{\boldsymbol{x}}\tilde{\boldsymbol{x}}^{\mathrm{H}}\boldsymbol{P}_{\tilde{\boldsymbol{J}}}^{\perp}\boldsymbol{P}_{\tilde{\boldsymbol{H}}}^{\perp}\boldsymbol{P}_{\tilde{\boldsymbol{J}}}^{\perp}\tilde{\boldsymbol{x}}}. \tag{57}$$

Note that when no directional interference exists, $\boldsymbol{P}_{\tilde{\boldsymbol{J}}} = \boldsymbol{0}_{N\times N}$ and, hence, Eq. (57) reduces to

$$t_{\text{DN-AMF}} = \frac{\tilde{\boldsymbol{x}}^{\mathrm{H}}\boldsymbol{P}_{\tilde{\boldsymbol{H}}}\tilde{\boldsymbol{x}}}{\tilde{\boldsymbol{x}}^{\mathrm{H}}\tilde{\boldsymbol{x}}\tilde{\boldsymbol{x}}^{\mathrm{H}}\boldsymbol{P}_{\tilde{\boldsymbol{H}}}^{\perp}\tilde{\boldsymbol{x}}}, \tag{58}$$

which is the subspace generalization of the DN-AMF in [29].

3.3 Wald test-based detector

For complex circular parameter, the Wald test is [44]

$$t_{\mathrm{Wald}} = (\hat{\boldsymbol{\Theta}}_{r1} - \boldsymbol{\Theta}_{r0})^{\mathrm{H}}\left\{\left[\boldsymbol{I}^{-1}(\hat{\boldsymbol{\Theta}}_1)\right]_{\boldsymbol{\Theta}_r\boldsymbol{\Theta}_r}\right\}^{-1}(\hat{\boldsymbol{\Theta}}_{r1} - \boldsymbol{\Theta}_{r0}), \tag{59}$$

where $\hat{\boldsymbol{\Theta}}_{r1}$ is the MLE of $\boldsymbol{\Theta}_r$ under hypothesis H_1, $\boldsymbol{\Theta}_{r0}$ is the value of $\boldsymbol{\Theta}_r$ under hypothesis H_0, $\{[\boldsymbol{I}^{-1}(\hat{\boldsymbol{\Theta}}_1)]_{\boldsymbol{\Theta}_r\boldsymbol{\Theta}_r}\}^{-1}$ is the Schur complement of $\boldsymbol{I}_{\boldsymbol{\Theta}_s\boldsymbol{\Theta}_s}$ when $\boldsymbol{\Theta} = \hat{\boldsymbol{\Theta}}_1$, namely,

$$\left\{[\boldsymbol{I}^{-1}(\hat{\boldsymbol{\Theta}}_1)]_{\boldsymbol{\Theta}_r\boldsymbol{\Theta}_r}\right\}^{-1} = \left(\boldsymbol{I}_{\boldsymbol{\Theta}_r\boldsymbol{\Theta}_r} - \boldsymbol{I}_{\boldsymbol{\Theta}_r\boldsymbol{\Theta}_s}\boldsymbol{I}_{\boldsymbol{\Theta}_s\boldsymbol{\Theta}_s}^{-1}\boldsymbol{I}_{\boldsymbol{\Theta}_s\boldsymbol{\Theta}_r}\right)\Big|_{\boldsymbol{\Theta}=\hat{\boldsymbol{\Theta}}_1}. \tag{60}$$

In a manner similar to the derivation of (37), we have

$$\left\{[\boldsymbol{I}^{-1}(\boldsymbol{\Theta})]_{\boldsymbol{\Theta}_r\boldsymbol{\Theta}_r}\right\}^{-1} = \boldsymbol{H}^{\mathrm{H}}(\boldsymbol{R} + \boldsymbol{q}\boldsymbol{q}^{\mathrm{H}})^{-1}\boldsymbol{H}. \tag{61}$$

Substituting (61) into (59) and using $\boldsymbol{\Theta}_r = \boldsymbol{\theta}$ and $\boldsymbol{\Theta}_{r0} = \boldsymbol{0}_{p\times 1}$, we obtain the Wald test with $\boldsymbol{\theta}$, $\boldsymbol{R}$, and $\boldsymbol{q}$ given

$$t_{\mathrm{Wald}_{\theta,\boldsymbol{R},\boldsymbol{q}}} = \boldsymbol{\theta}^{\mathrm{H}}\boldsymbol{H}^{\mathrm{H}}(\boldsymbol{R} + \boldsymbol{q}\boldsymbol{q}^{\mathrm{H}})^{-1}\boldsymbol{H}\boldsymbol{\theta}. \tag{62}$$

To derive the final Wald test, we need to obtain the MLEs of $\boldsymbol{\theta}$, $\boldsymbol{q}$ and $\boldsymbol{R}$ under hypothesis H_1.

Using (12) and (13), we obtain the following result under hypothesis H_1:

$$\hat{\boldsymbol{q}}_1 = \gamma_1 \boldsymbol{x}_1, \tag{63}$$

where $\boldsymbol{x}_1 = \boldsymbol{x} - \boldsymbol{H}\boldsymbol{\theta} - \boldsymbol{J}\boldsymbol{\phi}$ and γ_1 satisfies

$$|\gamma_1|^2 = \frac{\boldsymbol{x}_1^{\mathrm{H}} \hat{\boldsymbol{R}}_1^{-1} \boldsymbol{x}_1 - 1}{\boldsymbol{x}_1^{\mathrm{H}} \hat{\boldsymbol{R}}_1^{-1} \boldsymbol{x}_1}. \tag{64}$$

According to (63) and (64), we have

$$\begin{aligned}(\hat{\boldsymbol{R}}_1 + \hat{\boldsymbol{q}}_1 \hat{\boldsymbol{q}}_1^{\mathrm{H}})^{-1} &= \left[\hat{\boldsymbol{R}}_1 + \boldsymbol{x}_1 \boldsymbol{x}_1^{\mathrm{H}} - \frac{\boldsymbol{x}_1 \boldsymbol{x}_1^{\mathrm{H}}}{\boldsymbol{x}_1^{\mathrm{H}} \hat{\boldsymbol{R}}_1^{-1} \boldsymbol{x}_1}\right]^{-1} \\ &= \left[\hat{\boldsymbol{R}}_{1+} - \frac{\boldsymbol{x}_1 \boldsymbol{x}_1^{\mathrm{H}}}{\boldsymbol{x}_1^{\mathrm{H}} \hat{\boldsymbol{R}}_1^{-1} \boldsymbol{x}_1}\right]^{-1} \\ &= \hat{\boldsymbol{R}}_{1+}^{-1} + \frac{\hat{\boldsymbol{R}}_{1+}^{-1} \boldsymbol{x}_1 \boldsymbol{x}_1^{\mathrm{H}} \hat{\boldsymbol{R}}_{1+}^{-1}}{\boldsymbol{x}_1^{\mathrm{H}} \hat{\boldsymbol{R}}_1^{-1} \boldsymbol{x}_1 - \boldsymbol{x}_1^{\mathrm{H}} \hat{\boldsymbol{R}}_{1+}^{-1} \boldsymbol{x}_1},\end{aligned} \tag{65}$$

where

$$\hat{\boldsymbol{R}}_{1+} = \hat{\boldsymbol{R}}_1 + \boldsymbol{x}_1 \boldsymbol{x}_1^{\mathrm{H}}. \tag{66}$$

It is easy to verify that

$$\hat{\boldsymbol{R}}_{1+}^{-1} = \hat{\boldsymbol{R}}_1^{-1} - \frac{\hat{\boldsymbol{R}}_1^{-1} \boldsymbol{x}_1 \boldsymbol{x}_1^{\mathrm{H}} \hat{\boldsymbol{R}}_1^{-1}}{1 + \boldsymbol{x}_1^{\mathrm{H}} \hat{\boldsymbol{R}}_1^{-1} \boldsymbol{x}_1}. \tag{67}$$

It follows that

$$\hat{\boldsymbol{R}}_{1+}^{-1} \boldsymbol{x}_1 = \frac{\hat{\boldsymbol{R}}_1^{-1} \boldsymbol{x}_1}{1 + \boldsymbol{x}_1^{\mathrm{H}} \hat{\boldsymbol{R}}_1^{-1} \boldsymbol{x}_1}. \tag{68}$$

Substituting (67) and (68) into (65), after some algebra, we have

$$\begin{aligned}(\hat{\boldsymbol{R}}_1 + \hat{\boldsymbol{q}}_1 \hat{\boldsymbol{q}}_1^{\mathrm{H}})^{-1} &= \hat{\boldsymbol{R}}_1^{-1} - \frac{\hat{\boldsymbol{R}}_1^{-1} \boldsymbol{x}_1 \boldsymbol{x}_1^{\mathrm{H}} \hat{\boldsymbol{R}}_1^{-1}}{1 + \boldsymbol{x}_1^{\mathrm{H}} \hat{\boldsymbol{R}}_1^{-1} \boldsymbol{x}_1} + \frac{\hat{\boldsymbol{R}}_1^{-1} \boldsymbol{x}_1 \boldsymbol{x}_1^{\mathrm{H}} \hat{\boldsymbol{R}}_1^{-1}}{(1 + \boldsymbol{x}_1^{\mathrm{H}} \hat{\boldsymbol{R}}_1^{-1} \boldsymbol{x}_1)(\boldsymbol{x}_1^{\mathrm{H}} \hat{\boldsymbol{R}}_1^{-1} \boldsymbol{x}_1)^2} \\ &= \hat{\boldsymbol{R}}_1^{-1} - \frac{\boldsymbol{x}_1^{\mathrm{H}} \hat{\boldsymbol{R}}_1^{-1} \boldsymbol{x}_1 - 1}{(\boldsymbol{x}_1^{\mathrm{H}} \hat{\boldsymbol{R}}_1^{-1} \boldsymbol{x}_1)^2} \hat{\boldsymbol{R}}_1^{-1} \boldsymbol{x}_1 \boldsymbol{x}_1^{\mathrm{H}} \hat{\boldsymbol{R}}_1^{-1}.\end{aligned} \tag{69}$$

It follows from (15) that

$$\hat{\boldsymbol{R}}_1^{-1} \boldsymbol{x}_1 = L \boldsymbol{S}^{-1} \boldsymbol{x}_1. \tag{70}$$

Substituting (15) and (70) into (69) leads to

$$(\hat{\boldsymbol{R}}_1 + \hat{\boldsymbol{q}}_1 \hat{\boldsymbol{q}}_1^{\mathrm{H}})^{-1} = (L+1)\boldsymbol{S}^{-1} - (L+1)\frac{\boldsymbol{S}^{-1} \boldsymbol{x}_1 \boldsymbol{x}_1^{\mathrm{H}} \boldsymbol{S}^{-1}}{\boldsymbol{x}_1^{\mathrm{H}} \boldsymbol{S}^{-1} \boldsymbol{x}_1} + \frac{\boldsymbol{S}^{-1} \boldsymbol{x}_1 \boldsymbol{x}_1^{\mathrm{H}} \boldsymbol{S}^{-1}}{(\boldsymbol{x}_1^{\mathrm{H}} \boldsymbol{S}^{-1} \boldsymbol{x}_1)^2}. \tag{71}$$

Substituting (71) into (62) results in the Wald test for given θ

$$\begin{aligned}t_{\mathrm{Wald}_{\boldsymbol{\theta}}} =& (L+1)\boldsymbol{\theta}^{\mathrm{H}} \boldsymbol{H}^{\mathrm{H}} \boldsymbol{S}^{-1} \boldsymbol{H} \boldsymbol{\theta} - (L+1)\frac{|\boldsymbol{\theta}^{\mathrm{H}} \boldsymbol{H}^{\mathrm{H}} \boldsymbol{S}^{-1} \boldsymbol{x}_1|^2}{\boldsymbol{x}_1^{\mathrm{H}} \boldsymbol{S}^{-1} \boldsymbol{x}_1} + \frac{|\boldsymbol{\theta}^{\mathrm{H}} \boldsymbol{H}^{\mathrm{H}} \boldsymbol{S}^{-1} \boldsymbol{x}_1|^2}{(\boldsymbol{x}_1^{\mathrm{H}} \boldsymbol{S}^{-1} \boldsymbol{x}_1)^2} \\ =& (L+1)\boldsymbol{\theta}^{\mathrm{H}} \tilde{\boldsymbol{H}}^{\mathrm{H}} \tilde{\boldsymbol{H}} \boldsymbol{\theta} - (L+1)\frac{|\boldsymbol{\theta}^{\mathrm{H}} \tilde{\boldsymbol{H}}^{\mathrm{H}} \tilde{\boldsymbol{x}_1}|^2}{\tilde{\boldsymbol{x}_1}^{\mathrm{H}} \tilde{\boldsymbol{x}_1}} + \frac{|\boldsymbol{\theta}^{\mathrm{H}} \tilde{\boldsymbol{H}}^{\mathrm{H}} \tilde{\boldsymbol{x}_1}|^2}{(\tilde{\boldsymbol{x}_1}^{\mathrm{H}} \tilde{\boldsymbol{x}_1})^2},\end{aligned} \tag{72}$$

where

$$\tilde{\boldsymbol{x}_1} = \tilde{\boldsymbol{x}} - \tilde{\boldsymbol{B}} \boldsymbol{\varphi}. \tag{73}$$

Note that the Wald test in (72) is dependent on $\boldsymbol{\phi}$, since Eq. (73) implicitly depends on $\boldsymbol{\phi}$. In the following, we derive the MLEs of $\boldsymbol{\theta}$ and $\boldsymbol{\phi}$ under hypothesis H_1. It is known from (24) that the MLE of $\boldsymbol{\theta}$ under hypothesis H_1 is the first p components of $\hat{\boldsymbol{\varphi}}_1$. It is easy to verify that

$$\boldsymbol{B}^{\mathrm{H}}\boldsymbol{S}^{-1}\boldsymbol{B}=\begin{bmatrix}\boldsymbol{H}^{\mathrm{H}}\boldsymbol{S}^{-1}\boldsymbol{H} & \boldsymbol{H}^{\mathrm{H}}\boldsymbol{S}^{-1}\boldsymbol{J}\\ \boldsymbol{J}^{\mathrm{H}}\boldsymbol{S}^{-1}\boldsymbol{H} & \boldsymbol{J}^{\mathrm{H}}\boldsymbol{S}^{-1}\boldsymbol{J}\end{bmatrix}. \tag{74}$$

Let

$$\boldsymbol{C}\triangleq\left(\boldsymbol{B}^{\mathrm{H}}\boldsymbol{S}^{-1}\boldsymbol{B}\right)^{-1}=\begin{bmatrix}\boldsymbol{C}_{11} & \boldsymbol{C}_{12}\\ \boldsymbol{C}_{21} & \boldsymbol{C}_{22}\end{bmatrix}. \tag{75}$$

According to the partitioned matrix inversion lemma, we have

$$\boldsymbol{C}_{11}=\left[\boldsymbol{H}^{\mathrm{H}}\boldsymbol{S}^{-1}\boldsymbol{H}-\boldsymbol{H}^{\mathrm{H}}\boldsymbol{S}^{-1}\boldsymbol{J}(\boldsymbol{J}^{\mathrm{H}}\boldsymbol{S}^{-1}\boldsymbol{J})^{-1}\boldsymbol{J}^{\mathrm{H}}\boldsymbol{S}^{-1}\boldsymbol{H}\right]^{-1} \tag{76}$$

and

$$\boldsymbol{C}_{12}=-\boldsymbol{C}_{11}\boldsymbol{H}^{\mathrm{H}}\boldsymbol{S}^{-1}\boldsymbol{J}(\boldsymbol{J}^{\mathrm{H}}\boldsymbol{S}^{-1}\boldsymbol{J})^{-1}. \tag{77}$$

According to (24), (75)–(77), we have

$$\begin{aligned}\hat{\boldsymbol{\theta}}_1&=\boldsymbol{C}_{11}\boldsymbol{H}^{\mathrm{H}}\boldsymbol{S}^{-1}\boldsymbol{x}+\boldsymbol{C}_{12}\boldsymbol{J}^{\mathrm{H}}\boldsymbol{S}^{-1}\boldsymbol{x}\\&=\left[\boldsymbol{H}^{\mathrm{H}}\boldsymbol{S}^{-1}\boldsymbol{H}-\boldsymbol{H}^{\mathrm{H}}\boldsymbol{S}^{-1}\boldsymbol{J}(\boldsymbol{J}^{\mathrm{H}}\boldsymbol{S}^{-1}\boldsymbol{J})^{-1}\boldsymbol{J}^{\mathrm{H}}\boldsymbol{S}^{-1}\boldsymbol{H}\right]^{-1}\\&\quad\cdot\left[\boldsymbol{H}^{\mathrm{H}}\boldsymbol{S}^{-1}\boldsymbol{x}-\boldsymbol{H}^{\mathrm{H}}\boldsymbol{S}^{-1}\boldsymbol{J}(\boldsymbol{J}^{\mathrm{H}}\boldsymbol{S}^{-1}\boldsymbol{J})^{-1}\boldsymbol{J}^{\mathrm{H}}\boldsymbol{S}^{-1}\boldsymbol{x}\right]\\&=\left(\tilde{\boldsymbol{H}}^{\mathrm{H}}\boldsymbol{P}_{\tilde{\boldsymbol{J}}}^{\perp}\tilde{\boldsymbol{H}}\right)^{-1}\tilde{\boldsymbol{H}}^{\mathrm{H}}\boldsymbol{P}_{\tilde{\boldsymbol{J}}}^{\perp}\tilde{\boldsymbol{x}}.\end{aligned} \tag{78}$$

Substituting (24) into (73) leads to

$$\tilde{\boldsymbol{x}}_1=\boldsymbol{P}_{\tilde{\boldsymbol{B}}}^{\perp}\tilde{\boldsymbol{x}}. \tag{79}$$

Substituting (78) and (79) into (72) results in the final Wald test

$$t_{\mathrm{Wald}}=\tilde{\boldsymbol{x}}^{\mathrm{H}}\boldsymbol{P}_{\tilde{\boldsymbol{H}}|\tilde{\boldsymbol{J}}}^{\mathrm{H}}\boldsymbol{P}_{\tilde{\boldsymbol{H}}|\tilde{\boldsymbol{J}}}\tilde{\boldsymbol{x}}, \tag{80}$$

where

$$\boldsymbol{P}_{\tilde{\boldsymbol{H}}|\tilde{\boldsymbol{J}}}=\tilde{\boldsymbol{H}}\left(\tilde{\boldsymbol{H}}^{\mathrm{H}}\boldsymbol{P}_{\tilde{\boldsymbol{J}}}^{\perp}\tilde{\boldsymbol{H}}\right)^{-1}\tilde{\boldsymbol{H}}^{\mathrm{H}}\boldsymbol{P}_{\tilde{\boldsymbol{J}}}^{\perp} \tag{81}$$

is the oblique projection onto $\langle\tilde{\boldsymbol{H}}\rangle$ along $\langle\tilde{\boldsymbol{J}}\rangle$, and in (80) we have used $\boldsymbol{P}_{\tilde{\boldsymbol{B}}}^{\perp}\tilde{\boldsymbol{H}}=\boldsymbol{0}_{N\times p}$.

Note that the Wald test in (80) is a generalization of the AOPD in [35], for which the signal subspace is constrained to have a dimension of one and no nonhomogeneity is considered.

4 Numerical examples

We evaluate the detection performance of the proposed detectors by Monte Carlo simulations for a scenario of airborne radar. Suppose the airborne radar contains N_s antenna elements, and each element transmits N_p pulses. Then we have $N=N_sN_p$. Define the signal-to-clutter-plus-noise ratio (SCNR) as

$$\rho_{\mathrm{s}}=\boldsymbol{\theta}^{\mathrm{H}}\boldsymbol{H}^{\mathrm{H}}\boldsymbol{R}^{-1}\boldsymbol{H}\boldsymbol{\theta}. \tag{82}$$

Similarly, the interference-to-noise ratio (INR) is defined as

$$\rho_{\mathrm{i}}=\boldsymbol{\phi}^{\mathrm{H}}\boldsymbol{J}^{\mathrm{H}}\boldsymbol{R}^{-1}\boldsymbol{J}\boldsymbol{\phi}. \tag{83}$$

To quantify the degree of nonhomogeneity, we introduce the quantity

$$\rho_{\mathrm{q}}=\boldsymbol{q}^{\mathrm{H}}\boldsymbol{R}^{-1}\boldsymbol{q}, \tag{84}$$

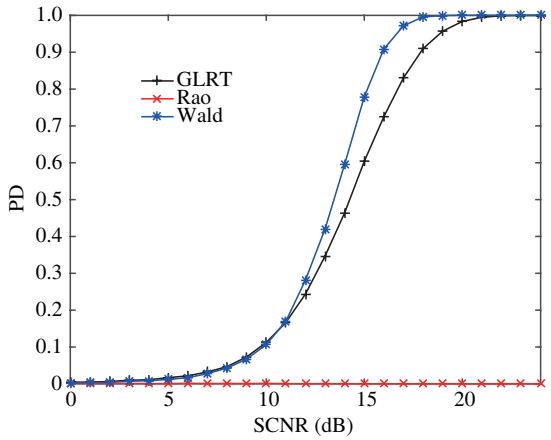

Figure 1 (Color online) PD versus SCNR. Here $N = 12$, $L = 2N$, $p = 2$, $r = 3$, $\rho_{\rm i} = 10$ dB, and $\rho_{\rm q} = 5$ dB.

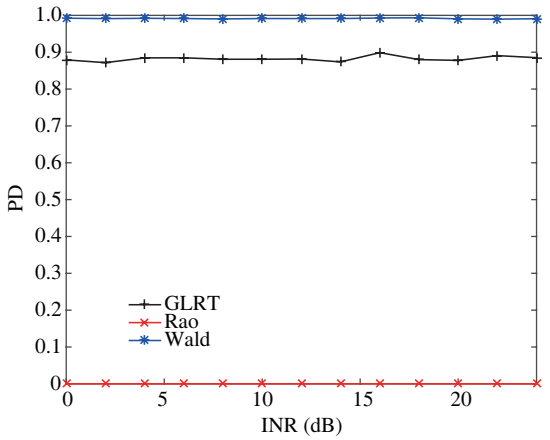

Figure 2 (Color online) PD versus INR. Here $N = 12$, $L = 2N$, $p = 2$, $r = 3$, $\rho_{\rm s} = 18$ dB, and $\rho_{\rm q} = 5$ dB.

which is referred to as the amount of covariance matrix mismatch.

We set the probability of false alarm (PFA) as PFA $= 10^{-3}$ in Figures 1–6. Figure 1 compares the detection performance of the proposed detectors under different SCNRs. The results show that the detection performance of the Wald test has the highest probability of detection (PD). In particular, the improvement of the Wald test with respect to the GLRT, in terms of SCNR, is roughly 2 dB when PD $= 0.9$. Moreover, for the chosen parameters, the Rao test is invalid.

Figure 2 displays the detection performance of the detectors under different INRs. It is seen that the PDs of the detectors are not affected by the change of the INR. In other words, the proposed detectors can effectively reject the directional interference.

Figure 3 plots the PDs of the detectors under different degrees of covariance matrix mismatch. It is shown that the PDs of the detectors all decrease when the covariance matrix mismatch increases. Hence, the nonhomogeneity property has a significant effect on the detection performance. Specifically, compared with the other two detectors, the GLRT is more robust to the nonhomogeneity. The PD of the GLRT decreases slower than that of the Wald test as the covariance matrix mismatch increases.

Note that in the above analysis, it is assumed that the actual signal completely lies within the assumed signal subspace. However, signal mismatch inevitably exists in practical applications, due to imperfect array calibration, multipath propagation, pointing errors, and so on [45, 46]. When signal mismatch occurs, the actual signal, denoted as $\boldsymbol{s}_0$, may not completely lie in the preassigned signal subspace spanned by the signal matrix $\boldsymbol{H}$. To measure the amount of signal mismatch, we resort to the quantity [47]

$$\cos^2\phi = \frac{\boldsymbol{s}_0^{\rm H}\boldsymbol{R}^{-1}\boldsymbol{H}(\boldsymbol{H}^{\rm H}\boldsymbol{R}^{-1}\boldsymbol{H})^{-1}\boldsymbol{H}^{\rm H}\boldsymbol{R}^{-1}\boldsymbol{s}_0}{\boldsymbol{s}_0^{\rm H}\boldsymbol{R}^{-1}\boldsymbol{s}_0}, \tag{85}$$

which is the cosine squared of the angle between the actual signal $\boldsymbol{s}_0$ and the nominal signal subspace spanned by $\boldsymbol{H}$ in the whitened space.

Figure 4 plots the PDs of the detectors under different degrees of signal mismatch. It is observed that the Wald test is much more robust than the GLRT.

Remarkably, the Rao test is invalid in Figures 1–4. However, when the system dimension (i.e., N) is large enough, the Rao test can provide high PD. The parameters used in Figure 5 are similar to Figure 1, but the value of N is much larger. The results in Figure 5 highlight that when N is large, the Rao test can provide a PD higher than 0.7. However, an apparent surprise result is that the PD of the Rao test is not a monotonically increasing function of the SCNR. Specifically, the PD of the Rao test first increases and then decreases, as the SCNR increases. This phenomenon is consistent with that in [37]. An intuitive explanation is that the Rao test criterion is originally proposed under the assumption of low SNR and a large number of training data.

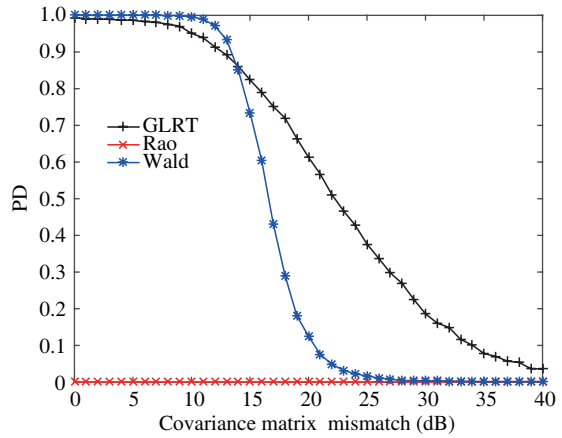

Figure 3 (Color online) PD versus covariance matrix mismatch. Here $N = 12$, $L = 2N$, $p = 2$, $r = 3$, $\rho_{\rm s} = 18$ dB, and $\rho_{\rm i} = 10$ dB.

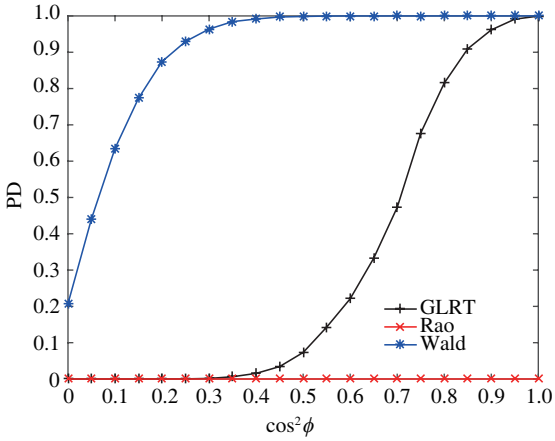

Figure 4 (Color online) PD versus degree of signal mismatch. Here $N = 12$, $L = 2N$, $p = 2$, $r = 3$, $\rho_{\rm s} = 22$ dB, $\rho_{\rm i} = 5$ dB, and $\rho_{\rm q} = 5$ dB.

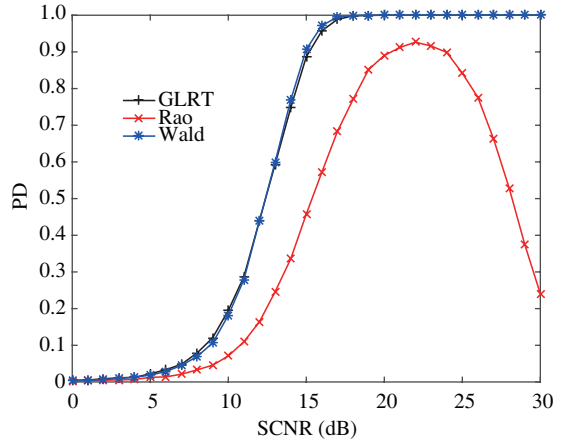

Figure 5 (Color online) PD versus SCNR. Here $N = 56$, $L = 2N$, $p = 2$, $r = 3$, $\rho_{\rm i} = 10$ dB, and $\rho_{\rm q} = 5$ dB.

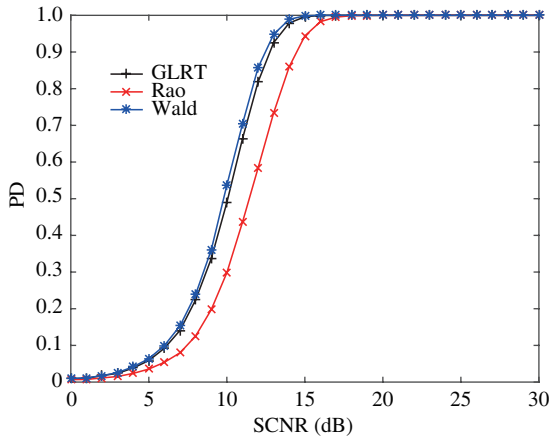

Figure 6 (Color online) PD versus SNR. Here $N = 56$, $L = 10N$, $p = 2$, $r = 3$, $\rho_{\rm i} = 10$ dB, and $\rho_{\rm q} = 5$ dB.

When the number of the training data is large enough, the PD of the Rao test recovers to behave as a monotonically increasing function of the SCNR. This is shown in Figure 6. Precisely, Figure 6 shows that when the system dimension and the number of training data is sufficiently large, the PD of the Rao test monotonically increases to 1 with the increase of the SCNR. However, the Rao test still suffers from a certain amount of performance loss, compared with the GLRT and Wald test. Precisely, the performance loss with respect to the Wald test is about 2 dB when PD = 0.9.

5 Conclusion

In this paper, we investigated the problem of detecting a multichannel signal in the presence of directional interference and structure nonhomogeneity. Three adaptive detectors were proposed according to the criteria of the GLRT, Rao test, and Wald test. It is shown that the proposed detectors can effectively reject the directional interference. However, the nonhomogeneity can severely affect the detection performance of the detectors. When the nonhomogeneity is not serious, the Wald test provides better performance than the other detectors. When the nonhomogeneity is serious, the GLRT performs the best. Moreover, the Wald test is most robust to signal mismatch. In addition, the Rao test has poor detection performance. In summary, if the nonhomogeneity is serious the GLRT is the best candidate. In other scenarios, the

Wald test would be the best choice.

Acknowledgements This work was supported by National Natural Science Foundation of China (Grant Nos. 61501505, 61501351).

Conflict of interest The authors declare that they have no conflict of interest.

References

1 Kelly E J. An adaptive detection algorithm. IEEE Trans Aerospace Electron Syst, 1986, 22: 115–127
2 Chen W S, Reed I S. A new CFAR detection test for radar. Digital Signal Process, 1991, 1: 198–214
3 Robey F C, Fuhrmann D R, Kelly E J, et al. A CFAR adaptive matched filter detector. IEEE Trans Aerospace Electron Syst, 1992, 28: 208–216
4 de Maio A. A new derivation of the adaptive matched filter. IEEE Signal Process Lett, 2004, 11: 792–793
5 de Maio A. Rao test for adaptive detection in Gaussian interference with unknown covariance matrix. IEEE Trans Signal Process, 2007, 55: 3577–3584
6 Pastina D, Lombardo P, Bucciarelli T. Adaptive polarimetric target detection with coherent radar part I: detection against Gaussian background. IEEE Trans Aerospace Electron Syst, 2001, 37: 1194–1206
7 Liu J, Zhang Z J, Yang Y. Optimal waveform design for generalized likelihood ratio and adaptive matched filter detectors using a diversely polarized antenna. Signal Process, 2012, 92: 1126–1131
8 Liu W J, Xie W C, Liu J, et al. Adaptive double subspace signal detection in Gaussian background—part I: homogeneous environments. IEEE Trans Signal Process, 2014, 62: 2345–2357
9 Xu J, Yu J, Peng Y N, et al. Radon-fourier transform for radar target detection. I: Generalized Doppler filter bank. IEEE Trans Aerospace Electron Syst, 2011, 47: 1186–1202
10 Xu J, Xia X G, Peng S B, et al. Radar maneuvering target motion estimation based on generalized Radon-Fourier transform. IEEE Trans Signal Process, 2012, 60: 6190–6201
11 Chen X, Guan J, Liu N B, et al. Maneuvering target detection via Radon-fractional Fourier transform-based long-time coherent integration. IEEE Trans Signal Process, 2014, 62: 939–953
12 Li X L, Cui G L, Yi W, et al. A fast maneuvering target detection motion parameters estimation algorithm based on ACCF. IEEE Signal Process Lett, 2015, 22: 270–274
13 Conte E, de Maio A, Ricci G. GLRT-based adaptive detection algorithms for range-spread targets. IEEE Trans Signal Process, 2001, 49: 1336–1348
14 Kraut S, Scharf L L. The CFAR adaptive subspace detector is a scale-invariant GLRT. IEEE Trans Signal Process, 1999, 47: 2538–2541
15 de Maio A, Iommelli S. Coincidence of the Rao test, Wald test, and GLRT in partially homogeneous environment. IEEE Signal Process Lett, 2008, 15: 385–388
16 Kraut S, Scharf L L. Adaptive subspace detectors. IEEE Trans Signal Process, 2001, 49: 1–16
17 Liu W J, Xie W C, Liu J, et al. Adaptive double subspace signal detection in Gaussian background—part II: partially homogeneous environments. IEEE Trans Signal Process, 2014, 62: 2358–2369
18 Rangaswamy M, Weiner D, Oeztuerk A. Non-Gaussian random vector identification using spherically invariant random processes. IEEE Trans Aerospace Electron Syst, 1993, 29: 111–124
19 Gini F, Farina A. Vector subspace detection in compound-Gaussian clutter part I: survey and new results. IEEE Trans Aerospace Electron Syst, 2002, 38: 1295–1311
20 Gini F. Sub-optimum coherent radar detection in a mixture of k-distributed and Gaussian clutter. IEEE Process, 1997, 144: 39–48
21 Gerlach K. Spatially distributed target detection in non-Gaussian clutter. IEEE Trans Aerospace Electron Syst, 1999, 35: 926–934
22 Cui G L, Kong L J, Yang X B, et al. Distributed target detection with polarimetric MIMO radar in compound-Gaussian clutter. Digital Signal Process, 2012, 22: 430–438
23 Sangston K J, Gini F, Greco M S. Coherent radar target detection in heavy-tailed compound-Gaussian clutter. IEEE Trans Aerospace Electron Syst, 2012, 64: 64–76
24 Zhang T X, Cui G L, Kong L J, et al. Phase-modulated waveform evaluation and selection strategy in compound-Gaussian clutter. IEEE Trans Signal Process, 2013, 61: 1143–1148
25 Zhang T X, Cui G L, Kong L J, et al. Adaptive Bayesian detection using MIMO radar in spatially heterogeneous clutter. IEEE Signal Process Lett, 2013, 20: 547–550
26 Kong L J, Li N, Cui G L, et al. Adaptive Bayesian detection for multiple-input multiple-output radar in compound-Gaussian clutter with random texture. IET Radar Sonar Navigation, 2016, 10: 689–698
27 Gao Y C, Li H B, Himed B. Knowledge-aided range-spread target detection for distributed MIMO radar in nonhomogeneous environments. IEEE Trans Signal Process, 2017, 65: 617–627
28 Besson O, Tourneret J Y, Bidon S. Knowledge-aided Bayesian detection in heterogeneous environments. IEEE Signal Process Lett, 2007, 14: 355–358
29 Orlando D, Ricci G. A Rao test with enhanced selectivity properties in homogeneous scenarios. IEEE Trans Signal Process, 2010, 58: 5385–5390

30 Besson O, Orlando D. Adaptive detection in nonhomogeneous environments using the generalized eigenrelation. IEEE Signal Process Lett, 2007, 14: 731–734
31 Hao C, Orlando D, Hou C. Rao and Wald tests for nonhomogeneous scenarios. Sensors, 2012, 12: 4730–4736
32 Bandiera F, Besson O, Orlando D, et al. GLRT-based direction detectors in homogeneous noise and subspace interference. IEEE Trans Signal Process, 2007, 55: 2386–2394
33 Bandiera F, Besson O, Ricci G. Direction detector for distributed targets in unknown noise and interference. Electron Lett, 2013, 49: 68–69
34 Liu W J, Liu J, Wang Y L, et al. Adaptive array detection in noise and completely unknown jamming. Digital Signal Process, 2015, 46: 41–48
35 Liu W J, Liu J, Hu X Q, et al. Statistical performance analysis of the adaptive orthogonal rejection detector. IEEE Signal Process Lett, 2016, 23: 873–877
36 Bandiera F, De Maio A, Greco A S, et al. Adaptive radar detection of distributed targets in homogeneous and partially homogeneous noise plus subspace interference. IEEE Trans Signal Process, 2007, 55: 1223–1237
37 Liu W J, Liu J, Huang L, et al. Rao tests for distributed target detection in interference and noise. Signal Process, 2015, 117: 333–342
38 Gao Y C, Liao G S, Liu W J. High-resolution radar detection in interference and nonhomogeneous noise. IEEE Signal Process Lett, 2016, 23: 1359–1363
39 Shuai X F, Kong L J, Yang J Y. Adaptive detection for distributed targets in Gaussian noise with Rao and Wald tests. Sci China Inf Sci, 2012, 55: 1290–1300
40 Hao C P, Orlando D, Ma X C, et al. Persymmetric Rao and Wald tests for partially homogeneous environment. IEEE Signal Process Lett, 2012, 19: 587–590
41 Liu J, Liu W J, Chen B, et al. Modified Rao test for multichannel adaptive signal detection. IEEE Trans Signal Process, 2016, 64: 714–725
42 Besson O. Detection in the presence of surprise or undernulled interference. IEEE Signal Process Lett, 2007, 14: 352–354
43 Yanai H, Takeuchi K, Takane Y. Projection Matrices, Generalized Inverse Matrices, and Singular Value Decomposition. New York: Springer, 2011
44 Liu W J, Wang Y L, Xie W C. Fisher information matrix, Rao test, and Wald test for complex-valued signals and their applications. Signal Process, 2014, 94: 1–5
45 Bandiera F, Besson O, Ricci G. An ABORT-like detector with improved mismatched signals rejection capabilities. IEEE Trans Signal Process, 2007, 56: 14–25
46 Hao C P, Liu B, Cai L. Performance analysis of a two-stage Rao detector. Signal Process, 2011, 91: 2141–2146
47 Liu W J, Liu J, Zhang C, et al. Performance prediction of subspace-based adaptive detectors with signal mismatch. Signal Process, 2016, 123: 122–126